Oncology
and Radiotherapy©
20(5) 2026 : 001-006 • RESEARCH ARTICLE

Development and Radiological Validation of Heterogeneous Pelvic Phantoms Against a Patient-Derived Distribution: A CT-Based Benchmarking Study of Rectal and Bladder Surrogates

Wiam EL ATIFI[1,2]*, Abdelali SLIMANI[1], Omar EL RHAZOUANI[1]

[1]Sciences and Engineering of Biomedicals, Biophysics and Health Laboratory, Higher Institute of Health Sciences, Hassan First University, Settat, 26000, Morocco
[2]Department of Radiotherapy, Hospital Center Ibn Rochd, Faculty of Medicine and Pharmacy, University Hassan II, Casablanca, Morocco

ABSTRACT

Background: Heterogeneous physical phantoms reproduce pelvic organ anatomy, yet their radiological representativeness at both whole-organ and wall-contour levels has not been evaluated against clinical CT data. This study benchmarks two heterogeneous phantoms — a polyurethane foam-walled rectal phantom and an epoxy-walled, water-filled bladder phantom — against 50 cervical cancer patients.

Materials and Methods: CT-derived mean Hounsfield unit (HU), electron density (ED), and volume were extracted from whole-rectum, rectal-wall, whole-bladder, and bladder-wall contours in 50 female patients (120 kVp, 400 mAs, 0.25 cm slice thickness) using the Elekta Monaco treatment planning system. Both phantoms were geometrically derived from an independent 200-patient average model and scanned under identical CT conditions. A three-tier percentile scoring framework (P25–P75: 2 points; P5–P95: 1 point; outside P5–P95: 0 points) was applied per parameter and contour (maximum 6 points per contour).

Results: For the rectal phantom, whole-rectum HU (−635 HU) and ED (0.446) deviated from patient medians by 15,975% and 56.0% respectively, falling below P5 at both contour levels; volumetric agreement was preserved (score: 2/6). For the bladder phantom, whole-bladder and bladder-wall HU and ED also fell below P5 — with smaller absolute deviations — while volume remained within the IQR (score: 2/6 per contour). Neither phantom achieved HU or ED representativeness at any contour level.

Conclusion: Geometric fidelity was successfully achieved by both designs, but material composition was the dominant limiting factor for radiological representativeness. Future heterogeneous pelvic phantom development should prioritise tissue-equivalent wall materials and optimised interface geometries to achieve both anatomical and radiological fidelity.

Keywords: Heterogeneous pelvic phantom; Rectal phantom; Bladder phantom; Polyurethane foam; Epoxy

Address for correspondence:
Wiam EL ATIFI,
Sciences and Engineering of Biomedicals, Biophysics and Health Laboratory,
Higher Institute of Health Sciences, Hassan First University,Settat, Morocco
Email: wiam98elatifi@gmail.com

Word count: 6298 **Tables:** 7 **References:** 23

Received: 02 May, 2026, Manuscript No. OAR-26-190252;
Editor assigned: 04 May, 2026, PreQC No. OAR-26-190252 (PQ);
Reviewed: 18 May, 2026, QC No. OAR-26-190252;
Revised: 23 May, 2026, Manuscript No. OAR-26-190252 (R);
Published: 30 May, 2026

INTRODUCTION

Anthropomorphic physical phantoms play a central role in radiation therapy quality assurance, serving as surrogate targets for dosimetric verification, imaging protocol development, and the commissioning of treatment planning systems [1,2]. In pelvic radiotherapy, accurate phantom representation of organ-specific radiological and mechanical properties is particularly critical, as dose gradients around structures such as the rectum and bladder can substantially influence both tumour control and normal tissue toxicity outcomes [3,4]. Both organs are primary organs at risk in the treatment of pelvic malignancies — including cervical, prostate, and rectal cancers — and demand phantom designs that faithfully replicate their Hounsfield unit (HU) distribution, electron density (ED), and anatomical geometry as observed under clinical computed tomography (CT) conditions.

The radiological properties of pelvic organs are inherently variable. Intraluminal content of the rectum — including gas, fluid, and stool — generates a wide range of HU values across clinical imaging datasets, complicating the task of constructing a single representative phantom [5]. Similarly, the bladder is not a simple fluid container; its CT appearance reflects the combined contributions of urine, wall tissue, partial-volume effects, and substantial inter-patient variability in filling status [6]. Tissue-mimicking materials (TMMs) developed for pelvic phantom applications must therefore reproduce this unique physiological behaviour while accommodating manufacturing constraints related to geometric precision, structural stability, and long-term reproducibility.

Several studies have established TMM formulations using epoxy resins and polyurethane-based materials for a wide range of organ and tissue types, and pelvic phantom designs have incorporated rectal and bladder surrogates — typically as silicone balloons, foam-filled cavities, or water-filled shells embedded within broader multi-organ constructs [7,8]. Epoxy resins are valued for their mechanical rigidity, chemical stability, and capacity to approximate soft-tissue density when appropriately formulated. Polyurethane foams, by contrast, offer greater flexibility and manufacturability and have been applied in geometrically complex anatomical surrogates [9,10]. These material families represent the two principal strategies in current heterogeneous pelvic phantom construction.

Despite the breadth of existing phantom development work, a precise and targeted gap remains unaddressed in the literature. Prior studies have incorporated rectal and bladder surrogates within broader pelvic phantom constructs, [11–14] but none has simultaneously resolved whole-organ and wall-contour levels as two distinct, independently characterised anatomical targets within a heterogeneous design, nor benchmarked CT-derived HU and ED values against organ-specific patient distributions for both organs. This gap is consequential: without validation at both contour levels, it is impossible to determine whether a given material choice is representative of the organ as a whole, of the wall specifically, or of neither — a distinction directly relevant to dose-volume histogram computation and organ-at-risk contouring practice in pelvic radiotherapy [15,16].

The present study addresses this gap by evaluating two heterogeneous pelvic phantom designs — a polyurethane foam-walled rectal phantom and an epoxy-walled, water-filled bladder phantom — against a clinical cohort of 50 pelvic cancer patients using a structured three-tier percentile scoring framework applied at both whole-organ and wall-contour levels. The study aims to determine whether heterogeneous phantom construction achieves radiological representativeness, and to provide evidence-based guidance for the material and design optimisation of future pelvic phantom systems.

MATERIALS AND METHODS

Patient Dataset

A total of 50 female patients diagnosed with cervical cancer were retrospectively and randomly selected for this study. The study was designed to evaluate the anatomical and radiological characteristics of both the rectum and bladder and was independent of treatment technique. All patients underwent CT simulation using a dedicated radiotherapy CT scanner following the institutional pelvic imaging protocol (120 kVp, 400 mAs, slice thickness 0.25 cm). Standard patient preparation procedures were applied, including instructions to maintain an empty rectum and a comfortably full bladder whenever possible; variations in organ filling were intentionally retained to reflect routine clinical conditions. Clinically approved whole-organ contours were available for all patients and were reviewed according to Radiation Therapy Oncology Group (RTOG) contouring recommendations [17]. Rectal-wall and bladder-wall contours were additionally generated within the treatment planning system (TPS) to permit separate analysis of wall-layer characteristics.

Development of Heterogeneous Phantoms

Two heterogeneous phantoms were fabricated and evaluated: a rectal phantom and a bladder phantom (Figure 1). Both were geometrically derived from an independent cohort of 200 patients, distinct from the study population. Segmentation was performed using 3D Slicer, and the resulting anatomical geometries were exported as stereolithography (STL) files for phantom fabrication.

For the heterogeneous rectal phantom (Figure 1a), the organ was designed as a hollow structure comprising a 5-mm-thick wall fabricated from polyurethane foam and an internal cavity containing air. This configuration was selected to reproduce the anatomical and density heterogeneity observed clinically within the rectum, where the wall constitutes a distinct soft-tissue layer surrounding an air- or content-filled lumen. Polyurethane-based materials have been employed in prior radiotherapy phantom construction due to their manufacturing flexibility and structural realism [10,11].

For the heterogeneous bladder phantom (Figure 1b), the bladder was constructed as a hollow shell comprising a 3-mm-thick wall fabricated from epoxy resin (DIPOXY-2K-700 EXPERT; 88% epoxy and 12% acetone by proportion) surrounding an internal cavity filled with water. This configuration was intended to reproduce the physiological distinction between the bladder muscular wall and the urine-equivalent lumen [9]. Water was selected as the cavity fill material because its radiological properties approximate those of urine and it is a widely used reference material in phantom dosimetry.

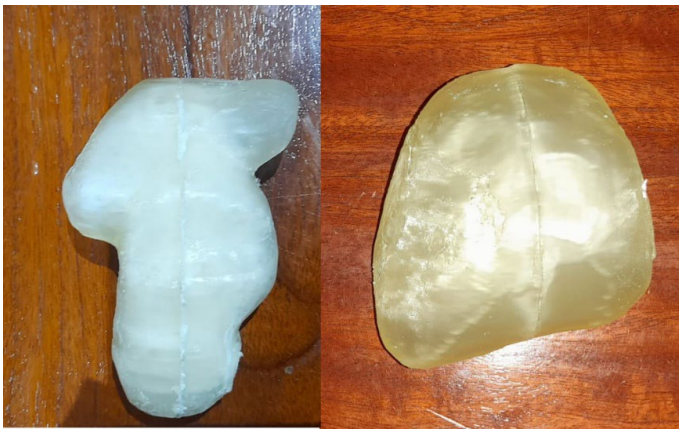

(a) (b)

Figure 1. Photographs of the fabricated heterogeneous pelvic phantoms: (a) rectal phantom comprising a 5-mm polyurethane foam wall surrounding an air-filled lumen, and (b) bladder phantom comprising a 3-mm epoxy resin shell surrounding a water-filled cavity.

Phantom CT Acquisition

Both phantoms were scanned using the same CT scanner and acquisition parameters applied to patient imaging (120 kVp, 400 mAs, slice thickness 0.25 cm). Phantoms were positioned within a composite attenuation assembly consisting of a multicube structure and bolus material to approximate patient-equivalent scattering conditions. A single CT acquisition was performed for each phantom. No image artefacts affecting quantitative analysis were observed.

CT Calibration and Electron Density Conversion

Conversion of HU values to ED was performed using the institution's clinically commissioned HU–ED calibration curve. The same calibration process was applied to all patient and phantom datasets. ED values were directly extracted from the TPS without additional processing.

Data Extraction

All measurements were performed within the Elekta Monaco TPS. Regions of interest included whole-rectum, rectal-wall,

whole-bladder, and bladder-wall contours for both patients and phantoms. For each structure, mean HU, mean ED, and volume were extracted using the TPS image statistics tools. Identical extraction and contouring procedures were employed across all datasets to ensure methodological consistency.

Statistical Analysis

Statistical analyses were performed using SPSS version 21.0. Descriptive statistics, including mean, median, standard deviation, range, minimum, and maximum, were calculated for all evaluated parameters. Normality of patient distributions was evaluated using the Shapiro–Wilk test.

To assess the clinical representativeness of each phantom, a percentile-based evaluation framework was applied. For each parameter (volume, HU, and ED), patient-derived percentile distributions were calculated, including the interquartile range (P25–P75) and the reference interval (P5–P95). A three-tier scoring system was then used to quantify phantom representativeness. Phantom values located within the IQR (P25–P75) were assigned 2 points, indicating strong representativeness of the central patient population. Values outside the IQR but within the P5–P95 reference interval were assigned 1 point, indicating acceptable but peripheral representativeness. Values falling outside P5–P95 were assigned 0 points, indicating non-representativeness of the observed patient population for that parameter. Scores were calculated independently for each parameter and contour type, yielding a maximum of 6 points per contour.

RESULTS

This table establishes the patient reference distributions against which both phantoms are subsequently benchmarked. The patient cohort exhibited substantial inter-individual variability across all organs and contour types. Whole-bladder HU and ED were tightly clustered (mean HU 5.04 ± 8.22; mean ED 1.010 ± 0.010), consistent with predominantly fluid-filled organ composition; bladder-wall HU showed considerably wider dispersion (SD 25.57 HU), reflecting heterogeneity in wall thickness and tissue composition. Whole-rectum HU was highly variable (mean −15.20 ± 57.29 HU; range 266 HU), reflecting the broad intraluminal variability introduced by gas, fluid, and stool, [5] yet the median of 4 HU and median ED of 1.013 confirm that the rectum, on average, behaves as a near-soft-tissue structure. The rectal wall showed a narrower HU range (247 HU) and higher median of 9.5 HU, consistent with predominantly soft-tissue wall composition when isolated from luminal contents. Volumetric variability was substantial for both organs — particularly the bladder (range 779.02 cc) — reinforcing the need for a percentile-based rather than mean-based reference framework for phantom evaluation.

Table 1: Descriptive statistics of CT-derived mean HU, mean ED, and volume for whole-bladder, bladder-wall, whole-rectum, and rectal-wall contours across the 50-patient clinical cohort.

Contour	Parameter	N	Mean	Median	Std. Dev.	Range	Min	Max
Whole Bladder	HU mean	50	5.04	3	8.22	33	−9.00	24
	ED mean		1.01	1.01	0.01	0.03	1	1.03
	Volume (cc)		279.27	236.47	174.72	779.02	72.18	851.2
Bladder Wall	HU mean		17.84	11	25.57	109	−11.00	98
	ED mean		1.02	1.02	0.01	0.04	1	1.03
	Volume (cc)		56.81	54.28	23.86	106.65	24.63	131.28
Whole Rectum	HU mean		−15.20	4	57.29	266	−229.00	37
	ED mean		0.99	1.01	0.06	0.31	0.74	1.04
	Volume (cc)		72.51	67.07	27.29	106.97	37.97	144.94
Rectum Wall	HU mean		−5.72	9.5	49.2	247	−212.00	35
	ED mean		1	1.02	0.05	0.23	0.81	1.04
	Volume (cc)		46.2	46.33	12.55	50.38	25.91	76.29

Table 2: Percentile-based zone classification of heterogeneous phantom CT measurements relative to the patient-derived reference interval (P5–P95) and interquartile range (P25–P75), for HU, ED, and volume across all contour types.

Contour	Parameter	P5–P95 Range	Median	Heterogeneous Phantom Value	Zone
Whole Bladder	HU mean	[−4.9, 21.25]	3	−6	Outside — Below P5
	ED mean	[1.0015, 1.0245]	1.009	1.001	Outside — Below P5
	Volume (cc)	[85.9, 780.2]	236.5	194.85	Inside IQR
Bladder Wall	HU mean	[−4.25, 93.7]	11	−13	Outside — Below P5
	ED mean	[0.9992, 1.0309]	1.015	0.996	Outside — Below P5
	Volume (cc)	[28.55, 119.84]	54.28	48.758	Inside IQR
Whole Rectum	HU mean	[−159.25, 34.0]	4	−635	Outside — Below P5
	ED mean	[0.863, 1.041]	1.013	0.446	Outside — Below P5
	Volume (cc)	[38.9, 128.97]	67.1	78.4	Inside IQR
Rectum Wall	HU mean	[−145.15, 34.45]	9.5	−370	Outside — Below P5
	ED mean	[0.873, 1.041]	1.018	0.653	Outside — Below P5
	Volume (cc)	[28.26, 71.84]	46.3	42.5	Inside IQR

This table is the core representativeness comparison for both heterogeneous phantoms. For the bladder phantom, the whole-bladder HU of −6 fell marginally below the P5 boundary of −4.9 HU, and the whole-bladder ED of 1.001 fell just below P5 (1.0015), placing both parameters outside the patient reference interval in the direction of underestimation. At the bladder-wall level, this pattern persisted: wall HU of −13 and wall ED of 0.996 were both below P5, whereas wall volume (48.758 cc) was comfortably inside the IQR. For the rectal phantom, the whole-rectum HU of −635 fell far below the P5 boundary of −159.25 HU — consistent with near-air rather than soft-tissue attenuation — and the corresponding ED of 0.446 fell dramatically below the clinical P5 of 0.863. At the rectal-wall level, the same radiological pattern persisted: wall HU of −370 and ED of 0.653 remained well outside the patient distribution, demonstrating that the polyurethane foam material itself — rather than the air-filled lumen — is the primary source of radiological non-representativeness. In both organs, volumetric measurements consistently fell within

the IQR, confirming that phantom geometry was clinically representative across all contour types.

Table 3: Absolute and percentage deviations of heterogeneous phantom HU, ED, and volume measurements from the patient population median, for all contour types.

Contour	Parameter	Patient Median	Heterogeneous Phantom Deviation (absolute; %)
Whole Bladder	HU mean	3	9 (300%)
	ED mean	1.009	0.008 (0.7%)
	Volume (cc)	236.5	41.7 (17.6%)
Bladder Wall	HU mean	11	24 (218%)
	ED mean	1.015	0.019 (1.9%)
	Volume (cc)	54.28	5.5 (10.2%)
Whole Rectum	HU mean	4	639 (15,975%)
	ED mean	1.013	0.567 (56.0%)
	Volume (cc)	67.1	11.3 (16.9%)
Rectum Wall	HU mean	9.5	379.5 (3,995%)
	ED mean	1.018	0.365 (35.9%)
	Volume (cc)	46.3	3.9 (8.3%)

This table quantifies the magnitude of the representativeness gaps identified in Table 2. For the bladder phantom, the HU deviations were modest in absolute terms: 9 HU (300%) for the whole bladder and 24 HU (218%) for the bladder wall. The ED deviations were negligible — 0.008 (0.7%) for the whole bladder and 0.019 (1.9%) for the bladder wall — indicating that the epoxy–water phantom construction produces radiological properties very close to, but systematically below, the patient distribution. Volumetric deviations were small (17.6% and 10.2% for whole-bladder and wall respectively), reflecting sound geometric fidelity. For the rectal phantom, the magnitude of deviation was dramatically greater: whole-rectum HU deviated by 639 HU (15,975%) and ED by 0.567 (56.0%) from their respective patient medians, reflecting the combined effect of air-void-laden polyurethane foam and an air-filled lumen. At the rectal-wall level — where luminal air no longer contributes — the HU deviation remained very large at 379.5 HU (3,995%) and ED deviation at 0.365 (35.9%), confirming that the foam wall material itself is the primary source of non-representativeness. Rectal volumetric deviations were modest (16.9% for the whole rectum; 8.3% for the wall), confirming that geometric accuracy was preserved despite extreme radiological deviation.

The scoring framework awards 2 points for a parameter falling within the IQR (P25–P75), 1 point for a value within P5–P95 but outside the IQR, and 0 points for values outside P5–P95 entirely. Both phantoms scored 2/6 for every evaluated contour, with all contributed points arising exclusively from volumetric representativeness — no score was achieved for HU or ED in any contour or organ. This uniform outcome across all four contour-phantom combinations demonstrates that geometric fidelity was consistently achieved by both designs, but that material-driven radiological representativeness was absent throughout. The low absolute scores confirm that neither heterogeneous phantom, in its current form, achieves adequate radiological representativeness for clinical dosimetric validation applications, and that material reformulation — particularly the substitution of polyurethane foam in the rectal phantom wall and optimisation of the bladder epoxy shell — is required before either design can be considered fully validated.

Table 4: Summary representativeness scores (maximum 6 points per contour) assigned to each heterogeneous phantom using the three-tier percentile-based scoring framework.

Contour	Heterogeneous Phantom Score	Summary
Whole Bladder	2/6	Volume inside IQR (2 pts); HU and ED below P5 (0 pts each)
Bladder Wall	2/6	Volume inside IQR (2 pts); HU and ED below P5 (0 pts each)
Whole Rectum	2/6	Volume inside IQR (2 pts); HU and ED below P5 (0 pts each)
Rectum Wall	2/6	Volume inside IQR (2 pts); HU and ED below P5 (0 pts each)

DISCUSSION

The present study evaluated the clinical representativeness of two heterogeneous pelvic phantoms — a polyurethane foam-walled rectal phantom and an epoxy-walled, water-filled bladder phantom — using a patient-distribution framework applied across four contour types in 50 cervical cancer patients. The findings consistently demonstrate that geometric realism, successfully achieved by both phantom designs, is insufficient to guarantee radiological representativeness: neither phantom reproduced clinically observed HU or ED distributions at any contour level.

A principal finding of this study is that the failure mechanism differs substantially between the two phantoms, reflecting the distinct material strategies employed in their construction. For the rectal phantom, the extreme radiological deviations — 15,975% for whole-rectum HU and 56.0% for ED — originate primarily from the physical properties of polyurethane foam. While polyurethane-based materials offer advantages in terms of manufacturability, structural flexibility, and anatomical realism, low-density foam contains a substantial fraction of air voids that dramatically reduce bulk density and electron density [10,19] As a result, the foam wall exhibits attenuation characteristics far closer to air than to soft tissue. The persistence of this pattern at the rectal-wall level — where luminal air no longer contributes — confirms that the foam material itself, not the air-filled lumen, is the dominant source of non-representativeness. The phantom thereby successfully reproduces the concept of a hollow rectum while simultaneously failing to reproduce the radiological environment that defines the organ during CT-based treatment planning.

For the bladder phantom, the failure mode was qualitatively different. The deviations were substantially smaller in absolute magnitude — 300% for whole-bladder HU and only 0.7% for ED — but were directionally consistent across both contour types: HU and ED were systematically underestimated below P5 in every case. For the whole-bladder contour, this underestimation is partly attributable to the water-filled lumen, whose radiological properties approximate those of urine and should theoretically benefit whole-organ representativeness. The fact that the measured whole-bladder HU of –6 fell only marginally below the P5 boundary of –4.9 HU suggests that the design concept was sound but requires modest recalibration [6,21]. At the wall level, the underestimation likely

reflects partial-volume averaging at the epoxy–water interface: when wall thickness approaches the dimensions of the imaging voxel, low-density contributions from the water-filled lumen are incorporated into wall measurements, reducing both measured HU and ED [13]. This effect is particularly relevant for bladder-wall analysis, where the physiological wall thickness of a distended bladder is only a few millimetres, and where accurate wall-specific radiological characterisation is essential for dose-response investigations.

The rectum presents a particularly challenging structure to model because its CT appearance is highly variable — rectal attenuation depends on varying proportions of soft tissue, stool, fluid, and intraluminal gas [5]. This physiological variability produces a broad range of HU values in clinical populations and complicates the definition of a single representative phantom. Nevertheless, despite this inherent variability, patient measurements remained clustered around soft-tissue-equivalent radiological properties, indicating that the rectum, when considered as a complete organ, behaves predominantly as a soft-tissue structure from a treatment-planning perspective. Consequently, successful phantom design requires materials capable of reproducing soft-tissue HU and ED characteristics rather than merely replicating geometric anatomy.

The comparison between whole-organ and wall-based analyses provides important insight into phantom validation methodology. Traditionally, validation studies have focused on whole-organ measurements, implicitly assuming that satisfactory agreement at the organ level implies adequate representation of clinically relevant substructures [20,21]. The present results demonstrate that this assumption may not always hold. Evaluating both contour types provides a more comprehensive understanding of phantom performance and enables identification of material-specific and geometry-specific limitations that may otherwise remain obscured by whole-organ analysis alone. Such a dual-contour approach is particularly relevant in radiotherapy, where dose-response relationships are increasingly investigated at the level of organ substructures — including the rectal wall and bladder wall — rather than entire organs [15,16].

The volumetric findings provide an additional and critical perspective on phantom design. Both phantoms consistently demonstrated acceptable geometric agreement with the patient cohort across all four contour types, confirming that the segmentation and model-generation workflow using 3D Slicer with an independent 200-patient average model successfully captured the characteristic anatomical dimensions of both organs [22-24]. The agreement observed for volume is particularly important because accurate organ dimensions constitute the foundation of anthropomorphic phantom design and directly influence contour-based dosimetric analyses. The decoupling of geometric fidelity from radiological representativeness observed here demonstrates that phantom validation cannot rely on geometric metrics alone — a multi-parameter framework that simultaneously evaluates HU, ED, and volume at both whole-organ and wall-contour levels provides a more sensitive and clinically relevant characterisation of phantom suitability.

Taken together, the results indicate that material selection is the primary determinant of radiological representativeness in heterogeneous pelvic phantom design. For the rectal phantom, replacing low-density foam with a tissue-equivalent wall material — such as epoxy resin formulated to produce soft-tissue-equivalent HU and ED values — would be the most direct route to achieving both the anatomical realism and radiological fidelity required for clinical dosimetric validation [9,18]. For the bladder phantom, increasing shell thickness or using a higher-density epoxy formulation may partially compensate for the partial-volume underestimation identified at the wall level. More broadly, multi-material designs capable of simultaneously reproducing wall-tissue and lumen-equivalent radiological characteristics represent the most promising direction for future heterogeneous pelvic phantom development [11,14].

CONCLUSION

This study demonstrated that two heterogeneous pelvic phantoms — a polyurethane foam-walled rectal phantom and an epoxy-walled, water-filled bladder phantom — achieved geometric representativeness but failed to reproduce clinically observed HU or ED distributions at any contour level, yielding a uniform representativeness score of 2/6 across all four evaluated contour types. The extreme radiological deviations of the rectal phantom (whole-rectum HU: 15,975% from patient median; ED: 56.0%) confirm that polyurethane foam is fundamentally incompatible with soft-tissue dosimetric requirements, while the systematic underestimation observed for the bladder phantom reflects partial-volume averaging at the epoxy–water interface. These findings establish that geometric realism alone is insufficient for clinical radiological representativeness, and that material composition is the dominant determinant of phantom suitability under CT-based treatment planning conditions. Future heterogeneous pelvic phantom development should therefore prioritise tissue-equivalent wall materials and interface geometries that preserve anatomical accuracy while reproducing the soft-tissue HU and ED characteristics required for accurate dosimetric validation in pelvic radiotherapy.

CONFLICT OF INTEREST STATEMENT

The authors declare no conflict of interest related to this study.

ETHICAL STATEMENT

Not applicable.

FUNDING

This research received no external funding.

REFERENCES

1. Abdollahi S, Mowlavi AA, Yazdi MHH, Ceberg S, Aznar MC, et al. Dynamic anthropomorphic thorax phantom for quality assurance of motion management in radiotherapy. Physics and Imaging in Radiation Oncology. 2024;30:100587.
2. Adib Y, Bouyhamarane A, Youssoufi MA, Drissi LB, Mesradi MR, et al. End-to-end patient-specific VMAT quality assurance for common head-and-neck cancers using RANDO anthropomorphic phantom with OSLD. Radiation Physics and Chemistry. 2025;230:112543.
3. Cheng XL, Liu JP, Wang BB, Sun L. Dosimetric comparison of coplanar and noncoplanar volumetric modulated arc therapy for ovarian-sparing cervical cancer radiation therapy. Journal of Radiation Research and Applied Sciences. 2025;18:101531.
4. Valencia Lozano I, Buss E, Spina CS, Horowitz DP, Kachnic LA, et al. Quantification and dosimetric impact of intra-fractional bladder changes during CBCT-guided online adaptive radiotherapy for pelvic cancer treatments. J Applied Clin Med Phys. 2025;26:e70074.
5. Faddegon B, Descovich M, Chen K, Ramos-Méndez J, Wahl N, et al. A digital male pelvis phantom series showing anatomical variations over the course of fractionated radiotherapy treatment. Medical Physics. 2024;51:3034-3044.
6. Sudhyadhom A. On the molecular relationship between Hounsfield Unit (HU), mass density, and electron density in computed tomography (CT). PLoS ONE. 2020;15:e0244861.
7. Hatamikia S, Jaksa L, Kronreif G, Birkfellner W, Kettenbach J, et al. Silicone phantoms fabricated with multi-material extrusion 3D printing technology mimicking imaging properties of soft tissues in CT. Zeitschrift für Medizinische Physik. 2025;35:138-151.
8. Jin H, Lee SY, An HJ, Choi CH, Chie EK, et al. Development of an anthropomorphic multimodality pelvic phantom for quantitative evaluation of a deep-learning-based synthetic computed tomography generation technique. J Applied Clin Med Phys. 2022;23:e13644.
9. Khallouqi A, Halimi A, El Rhazouani O, Mesradi MR, El Mansouri K, et al. Comparing tissue-equivalent properties of polyester and epoxy resins with PMMA material using Gate/Geant4 simulation toolkit. Radiation Physics and Chemistry. 2024;220:111702.
10. Vakil AU, Petryk NM, Du C, Howes B, Stinfort D, et al. In vitro and in vivo degradation correlations for polyurethane foams with tunable degradation rates. J Biomedical Materials Res. 2023;111:580-595.
11. Cunningham JM, Barberi EA, Miller J, Kim JP, Glide-Hurst CK. Development and evaluation of a novel MR-compatible pelvic end-to-end phantom. J Applied Clin Med Phys. 2019;20:265-275.
12. Katake A, Kumar L, Singh B, Haraniya K, Vashistha R, et al. Developing an indigenous anthropomorphic heterogeneous female pelvic phantom for dosimetric audit in radiotherapy centers. Journal of Cancer Research and Therapeutics. 2025;21:678-685.
13. Fernandez SV, Kim J, Sadat D, Marcus C, Suh E, et al. A dynamic ultrasound phantom with tissue-mimicking mechanical and acoustic properties. Advanced Science. 2024;11:2400271.
14. Yadav N, Singh M, Mishra SP, Ansari S. Development of an anthropomorphic heterogeneous female pelvic phantom and its comparison with a homogeneous phantom in advance radiation therapy: Dosimetry analysis. Medical Sciences. 2023;11:59.
15. Bouzaki A, Green D, Van Herk M, Shortall J, Puri T, et al. New rectum dose surface mapping methodology to identify rectal subregions associated with toxicities following prostate cancer radiotherapy. Physics and Imaging in Radiation Oncology. 2025;33:100701.
16. Desrochers A, Ghosh S, Parliament M, Garraway R, Kellogg L, Larocque MP. Comparison of dose statistics for bladder wall and rectum wall vs whole organs for VMAT prostate treatment. Medical Dosimetry. 2020;45:140-148.
17. Raina P, Singh S, Gurjar OP. Dosimetric study of indigenously developed heterogeneous pelvic phantom for radiotherapy quality assurance. Iran J Med Phys. 2019.
18. Ashour NI, Abdul Hadi MFR, Hashikin NAbA, Dheyab MA, Musa AS, et al. Investigating the suitability of newly developed epoxy-based equivalent tissues for newborn and 5-year-old in paediatric radiology. Radiation Physics and Chemistry. 2024;214:111288.
19. Badiuk SR, Sasaki DK, Rickey DW. An anthropomorphic maxillofacial phantom using 3-dimensional printing, polyurethane rubber and epoxy resin for dental imaging and dosimetry. Dentomaxillofacial Radiology. 2022;51:20200323.
20. Brand DH, Brüningk SC, Wilkins A, Naismith O, Gao A, et al. Gastrointestinal toxicity prediction not influenced by rectal contour or dose-volume histogram definition. Int J Radiat Oncol Biol Phys. 2023;117:1163-1173.
21. Herczeg BT, Sudár Á, Ortutay R, Ágoston P, Major T, et al. Risk estimations of radiation induced malignancies in rectum and bladder following radiotherapy of prostate carcinoma. Physica Medica. 2026;142:105714.
22. Fischer J, Fischer LA, Bensberg J, Bojko N, Bouabdallaoui M, et al. CBCT-based online adaptive radiotherapy of the bladder — geometrical and dosimetrical considerations compared to conventional IGRT. Radiat Oncol. 2025;20:128.
23. Gao X, Ge L, Gao J, Cao Z. Multiscale spatial relationship-based model for predicting bladder wall dose in pelvic radiotherapy. J Applied Clin Med Phys. 2024;25:e14153.
24. Willigenburg T, Van Der Velden JM, Zachiu C, Teunissen FR, Lagendijk JJW, et al. Accumulated bladder wall dose is correlated with patient-reported acute urinary toxicity in prostate cancer patients treated with stereotactic, daily adaptive MR-guided radiotherapy. Radiotherapy and Oncology. 2022;171:182-188.